

MUON-PROTON INELASTIC SCATTERING, $|q^2|$ LESS THAN $1.2 (\text{GeV}/c)^2$ *

B. D. Dieterle, T. Braunstein, J. Cox, F. Martin,
W. T. Toner, M. L. Perl, and T. F. Zipf
Stanford Linear Accelerator Center
Stanford University, Stanford, California 94305

W. L. Lakin
High Energy Physics Laboratory
Stanford University, Stanford, California 94305

H. C. Bryant
Physics Department
University of New Mexico, Albuquerque, New Mexico 87106

ABSTRACT

The inelastic scattering of muons has been measured using positive muons of $10 \text{ GeV}/c$ incident upon a liquid hydrogen target. Values of the differential cross section and of the virtual photon-proton absorption cross section for $|q^2|$ in the range of 0.05 to $1.2 (\text{GeV}/c)^2$ and for equivalent photon laboratory energies of 0.6 to 6.5 GeV , are presented.

*Work supported by the U. S. Atomic Energy Commission.

This is a preliminary report of the results of an extensive series of measurements of the muon elastic and inelastic cross sections using muons with momenta of 10 and 12 GeV/c. This experiment is the first measurement of the inelastic scattering of muons from pure hydrogen.¹ One purpose of this experiment is to investigate the virtual photon-proton interaction in these inelastic processes and this is the subject of this letter. The cross sections presented below were obtained using 10 GeV/c muons and are restricted to $0.05 \leq |q^2| \leq 1.2 \text{ (GeV/c)}^2$. In subsequent publications, cross sections for values of $|q^2|$ up to 3 (GeV/c)^2 will be given, and comparisons between muon-proton and electron-proton interactions will be made. The data from the entire experiment contain approximately 40 times as many events in the $|q^2| \geq 0.75 \text{ (GeV/c)}^2$ category as are presented here.

The source of muons for this experiment was the SLAC high energy muon facility. This beam² yields up to 10^5 muons per second in a phase space volume of $3 \times 10^{-3} \text{ cm}^2 \text{ sr}$ in a momentum band of ± 1.5 percent. The optical system of the beam contains two stages of momentum analysis and produces an almost dispersion free beam at the scattering target. The size of the beam at this point is 10 cm by 7 cm. At production, the ratio of pions to muons is approximately 0.3, but is reduced to 3×10^{-6} by placing a 5.5 m Be filter immediately after the production target. Veto counters were placed around the beam in the last section before the scattering target, so that beam halo muons would not trigger the apparatus.

An elevation view of the experiment is shown in Fig. 1. The liquid hydrogen scattering target is 198 cm in length and 18 cm in diameter. This is followed by a small sweeping magnet to prevent numerous knock-on electrons that are produced in the hydrogen target from reaching the spark chambers and trigger counters in front of the 54-inch diameter analyzing magnet. Muons which scatter through an angle of more than 25 mrad are detected by three planes of counters.

The spark chamber trigger is derived from appropriate combinations of elements of these arrays, in anti-coincidence with the beam halo veto counters.

The array after the analyzing magnet is preceded by 26 inches of steel to reduce the number of non-muon triggers. The angle of the scattered muon is measured in the first two thin-plate spark chambers. The analyzing magnet and the first four spark chambers are employed to determine the momentum of the scattered muon. The uncertainty in the momentum of the scattered particles due to measurement errors is ± 1.9 percent at 10 GeV/c. The last four chambers are constructed with 1/2 inch thick aluminum plates and have 6.5 inch thick steel absorbers placed between them. This combination, in addition to the 26 inches of steel mentioned above, ensures that the scattered particle is a muon by rejecting strongly interacting particles with an efficiency of ~ 97 percent. The pictures have been scanned for scattered particles which interact in the thick-plate chambers or in the steel. The number of strongly interacting particles, from all sources, which have been incorrectly labeled as scattered muons is estimated to be less than 0.2 percent. The value of the beam momentum deduced from measurements of elastically scattered muons was consistent with the results of calculations based on magnetic measurements of the beam magnets. Our best estimate of the average momentum of the muons at the center of the hydrogen target is $9.95 \pm .05$ GeV/c.

The number of muons incident upon the scattering target was monitored by a set of five small counter telescopes placed in the beam. These telescopes counted approximately 3 percent of the total particle flux, and were positioned such that they were insensitive to small changes in the shape and position of the beam. This monitor was calibrated, at low beam intensities, against a set of larger counters which covered the entire cross-sectional area of the beam. The results of these calibrations were then extrapolated to higher intensities. Dead time effects in

this procedure were one to two percent, and contribute negligibly to the uncertainty in normalization. Dead time due to random veto counts was typically 15 percent for the data presented here. It was measured in several circuits in the monitor system and in the trigger system. Variations in the correction from circuit to circuit result in a normalization uncertainty from this source of ± 1 percent. Dead time effects in the trigger system were negligible. It is estimated that the muon flux is known to ± 3 percent.

The data presented here result from 7.8×10^8 muons incident upon the full hydrogen target. Empty target background subtraction runs were taken with 6.4×10^8 incident muons. The resulting photographs were scanned for events in which at least one track was present, both in the four chambers used to determine the momentum and angle of the scattered particle and, depending upon the trajectory of this particle, in at least one of the thick-plate chambers after the steel absorber. Roughly 30,000 photographs satisfied these criteria and were measured using the SLAC-NRI film measuring devices. The reconstructed tracks of the scattered muons were projected into the hydrogen target and the distance of closest approach to the target axis, within the target length, was computed. It was established that more than 99 percent of the events in the final sample of the data had distances of closest approach of ≤ 7 cm. The application of such a criterion allowed the rejection, with a high level of confidence, of photographs arising from triggers initiated by beam halo particles. In all, 1474 events were used for the results presented in this letter. The number of empty target background events which satisfied the "good event" criteria was 104.

The detection efficiency for the relevant final states was calculated by a Monte-Carlo technique which traced the scattered muon trajectories through the detection system. The results of these calculations have been used as weighting

factors for each event. Corrections made to the data for scanning and measuring inefficiencies were 2 percent.

The differential cross section $d^2\sigma/dq^2 dK$ is presented in Table I. The square of the four-momentum transfer from the muon is $|q^2|$; the momentum of the incident (scattered) muon is $p(p')$ and the energy $E(E')$, the last four quantities being defined in the laboratory system. The energy of the virtual photon in the laboratory is ν where $\nu = E - E'$. Following Hand,³ we define $K = \nu - |q^2|/2M$, where M is the proton mass. Photons, real or virtual, with the same value of K produce final hadronic states with the same invariant mass.

As with other electromagnetic processes, the differential cross section is large at small $|q^2|$, and decreases rapidly as $|q^2|$ increases. For a fixed $|q^2|$, the differential cross section decreases rapidly as K increases. In the data presented $K \geq 0.6$ GeV. This permits an unambiguous elimination of both the elastic scattering and first nucleon resonance events from this data. The data on elastic scattering and inelastic scattering with small K will be reported in a future publication. Inelastic lepton-nucleon scattering is thought to proceed via the one-photon exchange mechanism,³ as shown in Fig. 2. In the framework of this approximation, it is natural to express the differential cross section as a product of kinematic factors and virtual photon cross sections, $\sigma_T(q^2, K)$ and $\sigma_S(q^2, K)$. σ_T and σ_S , as first defined by Hand,³ may be thought of as the total cross sections for the interaction of transverse and scalar virtual photons with protons. Their definition depends on how the flux of the virtual photons is defined and we give the Hand formula below:

$$\begin{aligned}
 d^2\sigma/dq^2 dK &= \Gamma_T(q^2, K) \sigma_T(q^2, K) + \Gamma_S(q^2, K) \sigma_S(q^2, K) \\
 &= \Gamma_T(q^2, K) \left[\sigma_T(q^2, K) + \epsilon \sigma_S(q^2, K) \right]
 \end{aligned}
 \tag{1}$$

Γ_T and Γ_S are the virtual photon fluxes for transverse and scalar photons, respectively, and ϵ is the ratio of these fluxes. Following Hand:³

$$\Gamma_T = \left(\frac{\alpha}{2\pi |q^2|} \right) \left(\frac{K}{p^2} \right) \left(1 - \frac{2m^2}{|q^2|} + \frac{2EE' - |q^2|/2}{(E - E')^2 + |q^2|} \right) \quad (2)$$

$$\epsilon = \left(\frac{2EE' - |q^2|/2}{(E - E')^2 + |q^2|} \right) / \left(1 - \frac{2m^2}{|q^2|} + \frac{2EE' - |q^2|/2}{(E - E')^2 + |q^2|} \right) \quad (3)$$

Here m is the muon mass and the other quantities have been previously defined. The central value of ϵ is given in Table I for each bin and in most cases is close to 1.

These definitions require that as $|q^2|$ goes to zero, σ_T goes to the physical photon-proton total cross section and σ_S goes to zero. With the data in this paper we cannot separate σ_T from σ_S . Therefore, using Eqs. (1) and (2) we calculate the combination $(\sigma_T + \epsilon\sigma_S)$. For convenience we define $\sigma_{\text{exp}} = (\sigma_T + \epsilon\sigma_S)$. σ_{exp} is presented in Table I. Both the values of σ_{exp} and of $d^2\sigma/dq^2 dK$ are the average values in the indicated $|q^2|$ and K bins. The given errors are statistical only. We estimate the overall normalization uncertainty to be ± 6 percent, at present.

The cross sections have been corrected for radiative effects. The extent of the correction is indicated in Table I. The quantity given is the fraction by which the measured cross sections were reduced. This correction, which is dependent upon the scattering variables, includes the contributions from elastic scattering, the first nucleon resonance, and the inelastic continuum using the methods of Tsai.⁴ The largest contribution to this correction is the radiative tail of the elastic scattering. The continuum correction is always less than 4 percent.

For the convenience of the reader we give corresponding $\sigma_{\gamma p}$ values, the physical photon-proton total cross section, derived from bubble chamber measurements.^{5, 6, 7} In the following letter we shall compare the values of σ_{exp} in Table I with the prediction of several theoretical models and shall also make use of the $\sigma_{\gamma p}$ values.

We also present in Table I the differential cross section ($d\sigma/dK$) in each energy range for $|q^2|$ greater than 0.1 (GeV/c)^2 , obtained by integrating our data. The integrated cross section for $|q^2|$ greater than 0.1 (GeV/c)^2 and for K in the range of 0.6 to 6.5 GeV is 0.77 microbarns.

We wish to thank E. H. Bellamy for the conception and design of the beam monitor system and John C. Pratt for his assistance in running the experiment. We wish to thank our technicians and programmers and the staff of the Stanford Linear Accelerator Center for their help and patience during the experiment. We are particularly grateful to our scanners for their continued diligence and support.

REFERENCES

1. For recent measurements of inelastic muon scattering on carbon see C. M. Hoffman, A. D. Lieberman, E. Engels, Jr., D. C. Imrie, P. G. Innocenti, R. Wilson, C. Zajde, W. A. Blampied, D. G. Stairs, and D. Drickey, *Phys. Rev. Letters* 22, 659 (1969).
2. J. Cox, F. Martin, M. L. Perl, T. H. Tan, W. T. Toner, T. F. Zipf, and W. L. Lakin, *Nucl. Instr. and Methods* 69, 77 (1969).
3. L. N. Hand, *Phys. Rev.* 129, 1834 (1963).
4. Y. S. Tsai, Proceedings of Nucleon Structure Conference at Stanford, 1963, edited by R. Hofstadter and L. Schiff (Stanford University Press, Stanford, California, 1964); p. 221.
5. H. G. Hilpert, H. Schnackers, H. Weber, A. Meyer, A. Pose, J. Schreiber, K. Bockmann, E. Paul, E. Propach, H. Butenschon, H. Meyer, S. Rieker, H. Baisch, B. Naroska, O. Braun, P. Steffen, J. Stiewe, H. Wenninger, H. Finger, P. Schlamp, and P. Seyboth, *Phys. Letters* 27B, 474 (1968).
6. J. Ballam, G. B. Chadwick, R. Gearhart, Z.G.T. Guiragossian, P. R. Klein, A. Levy, M. Menke, J. J. Murray, P. Seyboth, G. Wolf, C. K. Sinclair, H. H. Bingham, W. B. Fretter, K. C. Moffeit, W. J. Podolsky, M. S. Rabin, A. H. Rosenfeld, and R. Windmolders, Report No. SLAC-PUB-618, Stanford Linear Accelerator Center, Stanford University, Stanford, California (1969) (unpublished).
7. J. Ballam, G. B. Chadwick, Z.G.T. Guiragossian, P. Klein, A. Levy, M. Menke, E. Pickup, T. H. Tan, P. Seyboth, and G. Wolf, *Phys. Rev. Letters* 21, 1541 (1968).

TABLE CAPTION

- I. 10 GeV/c muon-proton inelastic scattering cross sections. ϵ is the ratio of longitudinal to scalar "virtual photon flux;" Δ_{rad} is the radiative correction which has been applied to the data; $d^2\sigma/dq^2dK$ is the measured differential cross section and $d\sigma/dK$ is the integral of $d^2\sigma/dq^2dK$ over q^2 from 0.1 GeV/c² to the maximum presented in the Table; σ_{exp} is the "virtual photon-proton total cross section." The quantities listed under σ_{exp} corresponding to $q^2 = 0$ are experimental photon-proton total cross sections (see text) from Refs. 5, 6, and 7. σ_{exp} and $d^2\sigma/dq^2dK$ are overall averages for each bin with efficiencies and kinematic parameters folded into the average. Because of this, σ_{exp} cannot be calculated directly using the tabulated values of $d^2\sigma/dq^2dK$.

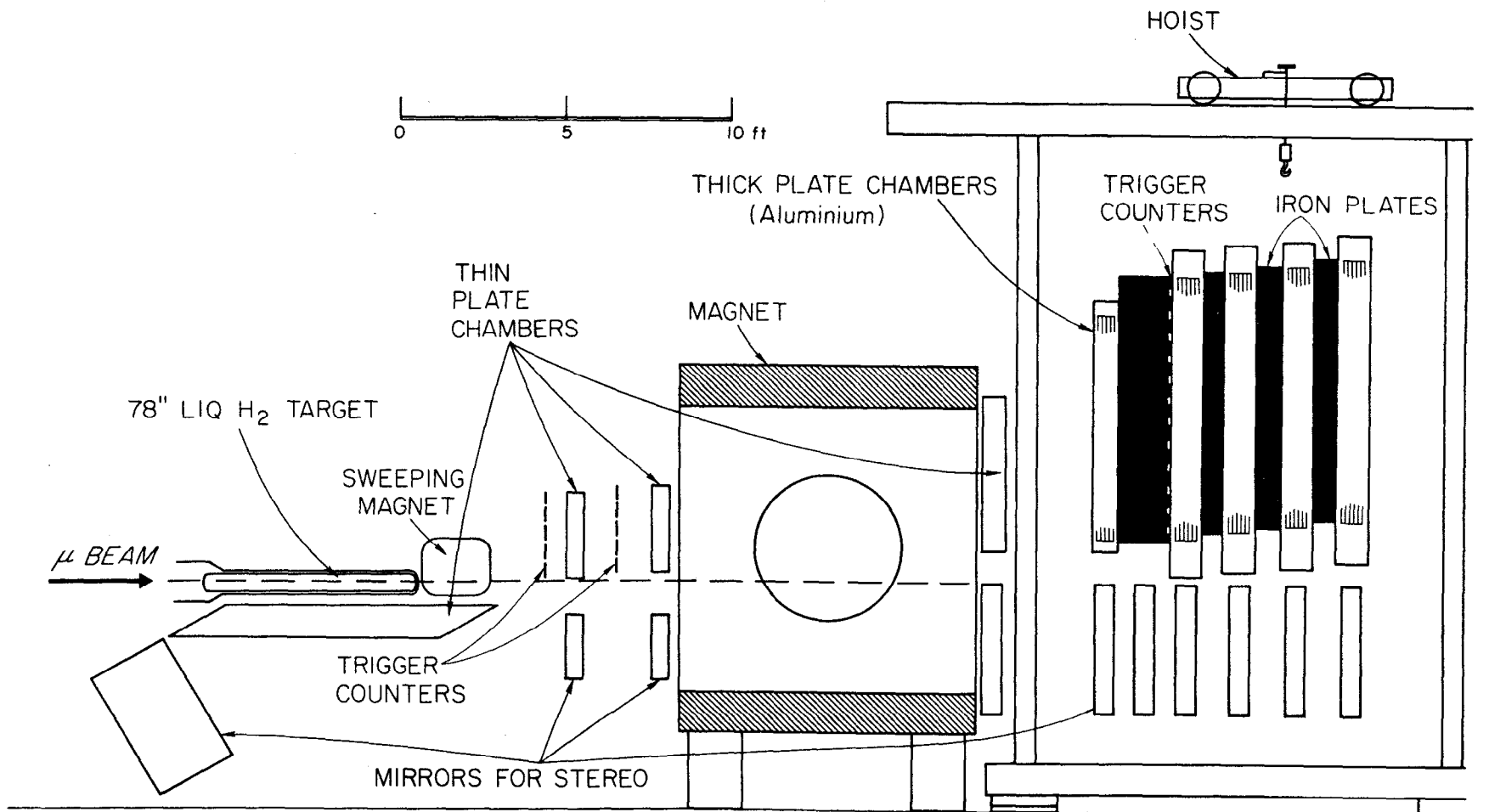
FIGURE CAPTIONS

1. Elevation view of the μ -p experimental setup.
2. One-photon exchange diagram for muon inelastic scattering.

TABLE I

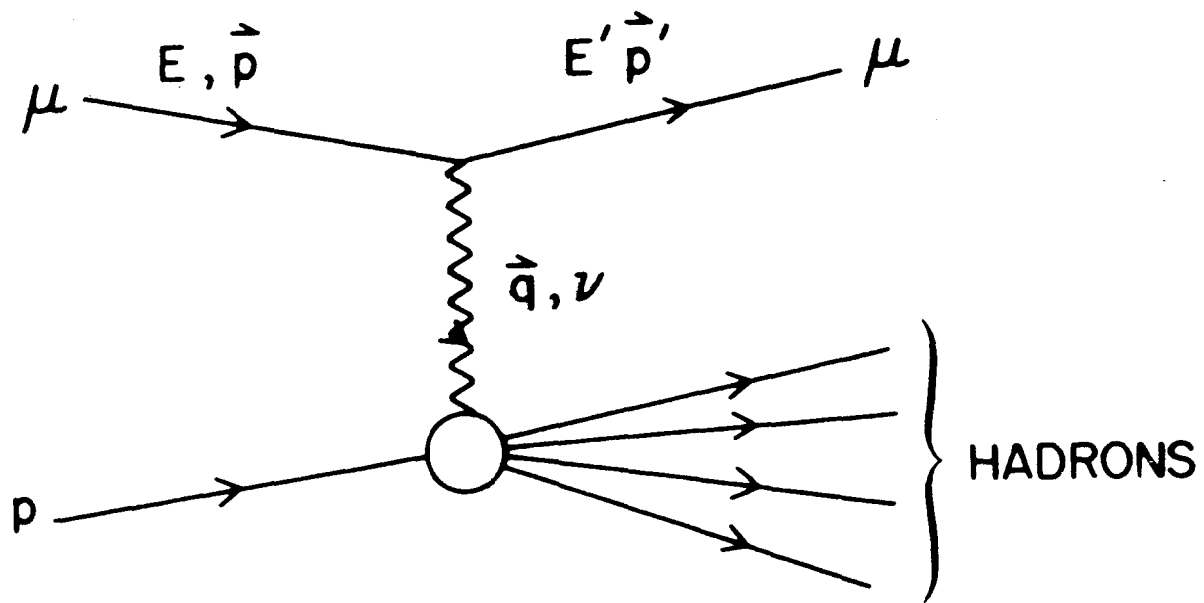
k GeV	$ q^2 $ GeV/c ²	ϵ	Δ_{RAD} %	$d\sigma/dK$ nb/GeV	$d^2\sigma/d q^2 dK$ nb/(GeV ³ /c ²)	σ_{exp} μb
0.6-1.0	0	-	-	-	-	201 ± 20
	.1 - .2	.99	4.0	489 ± 35	2140 ± 260	158 ± 19
	.2 - .4	.99	2.1		740 ± 78	144 ± 16
	.4 - .6	.99	0.2		322 ± 53	154 ± 26
	.6 - .8	.99	-0.8		167 ± 42	145 ± 36
	.8 - 1.2	.98	-1.4		73 ± 21	119 ± 36
1-2	0	-	-	-	-	151 ± 9
	.076 - .1	.99	5.0	250 ± 16	2820 ± 480	196 ± 33
	.1 - .2	.98	5.3		1100 ± 110	130 ± 13
	.2 - .4	.98	3.9		351 ± 33	101 ± 10
	.4 - .6	.98	3.0		175 ± 26	102 ± 15
	.6 - .8	.97	1.3		89 ± 23	100 ± 25
	.8 - 1.2	.97	0.6		43 ± 11	73 ± 19
2-3	0	-	-	-	-	134 ± 8
	.067 - .1	.96	6.8	116 ± 11	1510 ± 377	179 ± 43
	.1 - .2	.96	8.5		416 ± 64	89 ± 13
	.2 - .4	.95	5.8		179 ± 22	78 ± 10
	.4 - .6	.95	3.9		79 ± 19	72 ± 17
	.6 - .8	.94	3.3		42 ± 14	62 ± 22
	.8 - 1.2	.93	2.1		36 ± 11	84 ± 26
3-5	0	-	-	-	-	127 ± 8
	.0535 - .1	.88	12.8	75 ± 6	615 ± 137	125 ± 25
	.1 - .2	.87	10.2		282 ± 32	110 ± 12
	.2 - .4	.87	7.3		121 ± 14	96 ± 12
	.4 - .6	.86	6.1		48 ± 10	66 ± 15
	.6 - .8	.85	5.5		26 ± 9	55 ± 19
	.8 - 1.2	.83	4.3		19 ± 6	67 ± 22
5-6.5	0	-	-	-	-	125 ± 11
	.1 - .2	.71	16.5		137 ± 26	92 ± 17
	.2 - .4	.69	13.2		52 ± 13	65 ± 16
	.4 - .7	.68	11.5		16 ± 9	41 ± 24

76



544C1

Fig. 1



1412A1

Fig. 2